BMC Genomics

RESEARCH

Open Access

# Genome-wide identification and expression pattern analysis of *the cinnamoyl-CoA reductase* gene family in flax (*Linum usitatissimum* L.)

Xixia Song[1†], Dandan Liu[1†], Yubo Yao[1], Lili Tang[1], Lili Cheng[1], Lie Yang[1], Zhongjuan Jiang[1,2], Qinghua Kang[1], Si Chen[1], Jiarong Ru[1], Lili Zhang[1], Guangwen Wu[1] and Hongmei Yuan[1*]

## Abstract

**Background** Cinnamoyl-CoA reductase (CCR) is the first important and committed enzyme in the monolignol synthesis branch of the lignin biosynthesis (LB) pathway, catalyzing the conversion of cinnamoyl-CoAs to cinnamaldehydes and is crucial for the growth of *Linum usitatissimum* (flax), an important fiber crop. However, little information is available about CCR in flax (*Linum usitatissimum* L.).

**Results** In this study, we conducted a genome-wide analysis of the *CCR* gene family and identified a total of 22 *CCR* genes. The 22 *CCR* genes were distributed across 9 chromosomes, designated *LuCCR1-LuCCR22*. Multiple sequence alignment and conserved motif analyses revealed that LuCCR7/13/15/20 harbor completely conserved NADP-specific, NAD(P)-binding, and CCR signature motifs. Furthermore, each of these *LuCCRs* is encoded by 5 exons separated by 4 introns, a characteristic feature of functional *CCRs*. Phylogenetic analysis grouped LuCCRs into two clades, with LuCCR7/13/15/20 clustering with functional CCRs involved in LB in dicotyledonous plants. RNA-seq analysis indicated that *LuCCR13/20* genes are highly expressed throughout all flax developmental stages, particularly in lignified tissues such as roots and stems, with increased expression during stem maturation. These findings suggest that *LuCCR13/20* play crucial roles in the biosynthesis process of flax lignin. Additionally, *LuCCR2/5/10/18* were upregulated under various types of abiotic stress, highlighting their potential roles in flax defense-related processes.

**Conclusions** This study systematically analyzes the *CCR* gene family (CCRGF) of flax (*Linum usitatissimum* L.) at the genomic level for the first time, so as to select the whole members of the CCRGF of flax and to ascertain their potential roles in lignin synthesis. Therefore, in future work, we can target genetic modification of *LuCCR13/20* to optimize the content of flax lignin. As such, this research establishes a theoretical foundation for studying *LuCCR* gene functions and offers a new perspective for cultivating low-lignin flax varieties.

**Keywords** Flax *(Linum usitatissimum* L.*)*, *CCR*, Lignin biosynthesis, Abiotic stress, Expression patterns

[†]Xixia Song and Dandan Liu contributed equally to this work.

*Correspondence:
Hongmei Yuan
yuanhm1979@163.com
[1]Heilongjiang Academy of Agricultural Sciences, Harbin 150000, China
[2]Heilongjiang University, Harbin 150000, China

## Background

Flax *(Linum usitatissimum* L.*)* stands as a cornerstone cash crop valued for its multifaceted utility in linseed oil and flax fiber production. Fiber flax, a major morphotype of cultivated flax, represents the oldest domesticated crop and serves as a prime source of fiber for human consumption [1]. Renowned for their robust tensile strength and supple fine texture, flax fibers, derived from phloem, are ideal raw materials for the industrial production of premium-grade textiles [2, 3]. In recent years, the integration of flax fibers into composite materials has further expanded its applications across various industries, including automotive, aerospace and packaging [2, 4]. The flax industry in China is an important part of international trade. Currently, China is a major exporter of flax products worldwide, yet the flax fiber used in production is primarily imported. If we aim to enhance the economic benefits of Chinese flax fiber, it is imperative to develop our own raw material industry. Consequently, cultivating new varieties with high fiber yield and superior quality becomes urgent.

The chemical composition of flax fiber is mainly cellulose, followed by hemicellulose and lignin. Lignin, a complex organic polymer, constitutes a crucial component of plant secondary cell walls with a role in orchestrating numerous vitally important physiological processes related to plant defense, mechanical support and water transport [5, 6]. Lignin plays significant biological roles; however, it adversely affects the utilization of flax fibers. On the one hand, lignin is the most difficult component to remove in the degumming process of flax. The high lignin content impedes the flax degumming process and contributes to increased waste pollution during fiber processing [7–9]. On the other hand, the high lignin content leading to substantial variability in fiber structure and a coarser texture, impairing textile performance. Notably, raw flax lignin content significantly influences fiber quality, necessitating strategic lignin content modification to advance the flax industry.

Given lignan's pivotal role in plant growth and industrial applications, extensive studies have been conducted to elucidate lignin biosynthetic pathways. In flax, this pathway comprises two major branches: the monolignol-specific pathway, which converts hydroxycinnamoyl-CoAs into monolignols, and the phenylpropanoid pathway, which converts phenylalanine into hydroxycinnamoyl-CoAs [10–12]. Cinnamoyl-CoA reductase (CCR) is an enzyme which belongs to the SDR (short-chain dehydrogenase/reductase) superfamily and catalyzes the first step in the monolignol-specific pathway [13, 14]. Importantly, this pathway converts in total of five hydroxycinnamoyl-CoAs (5-hydroxyferuloyl-CoA, caffeoyl-CoA, feruloyl-CoA, p-coumaroyl-CoA and sinapoyl-CoA) into their corresponding cinnamaldehydes, which serve as precursors for lignin production [15–18]. Thus, CCR potentially regulates the carbon flux of the lignin synthesis pathway, making it an attractive target for interventions aimed at altering lignin levels [19].

Cinnamoyl-CoA reductase has been identified in many plants, with the number of family members varying, including *Arabidopsis thaliana* with 11 genes [20], *Populus tomentosa* with 11 genes [21], *Oryza sativa* with 33 genes [22], *Medicago sativa* with 30 genes [23], and *Eucalyptus grandis* with 10 genes [24]. Research on the functions of *CCR* genes has been conducted indiverse species, such as *A. thaliana* [25] and *O. sativa* [26], among others [27–30]. Intriguingly, downregulation of *AtCCR1* expression in *A. thaliana* reduced lignin content by up to 50% [25], while reintroduction of functional *CCR1* into *AtCCR1* mutants effectively prevented vascular collapse and increased total stem biomass by 59% compared to wild type (WT) [31]. Additionally, overexpression of *BnCCR1* and *BnCCR2* in *Brassica napus* were shown to increase lignin content both in stems and in roots [32]. Furthermore, transgenic *O. sativa* (rice) plants overexpressing *OsCCR10* exhibited high root lignin content, whereas the *OsCCR10* knock-out mutants mediated by CRISPR/Cas9 showed reduced lignin accumulation in root [26]. All of the above discoveries imply that regulating *CCR* gene expression may effectively alter lignin content in plants. However, there is little information on the identification and functional characterization of *CCRs* in flax. Therefore, it is necessary to conduct in-depth identification and analysis of the flax *CCR* gene family, to elucidate the structure-function relationships of these proteins.

The first flax genome was assembled in 2012, with different versions being published subsequently [33, 1–2, 4]. Thanks to the publication of the flax genome, numerous genes associated with key agronomic traits have been identified and utilized, significantly accelerating the process of flax molecular breeding [34, 35]. Genome-wide identification enable systematic characterization of key enzymes and their corresponding family members [36]. This study, which utilized flax genomic data, identified all members of the *CCR* gene family and further analyzed their gene structure, evolutionary relationships, and expression patterns, determining the key CCRs involved in the lignin synthesis process of flax. Genome-wide analysis offers valuable insights for selecting target genes for subsequent functional validation of *CCR*. A high lignin content increases the production cost of flax fiber raw materials. Targeted genetic modification of the *CCR* gene can reduce the lignin content, thereby lowering production costs.

This study systematically analyzes the *CCR* gene family (CCRGF) of flax (*Linum usitatissimum*) at the genomic

level for the first time, to ascertain their potential roles in lignin synthesis. As such, this research establishes a theoretical foundation for studying *LuCCR* gene functions and offers a new perspective for cultivating low-lignin flax varieties.

## Results

### Genome-wide identification and chromosomal localization of *LuCCRs*

Totally, 22 *CCR* genes were identified in *L. usitatissimum* through conserved domain confirmation and homology analyses focusing on the signature motif (KNWYCYGK). The sequence information of *LuCCRs* is shown in Supplementary Table 1. These genes were designated *LuCCR1* through *LuCCR22* based on their chromosomal locations, with detailed information provided in Table 1. Notably, LuCCR amino acid sequence lengths ranged from 275 to 593 aa, with the majority of LuCCRs (except for LuCCR3/9/13) exhibiting sequence lengths of approximately 300 aa, as consistent with known functional CCRs [37].

The investigated molecular weights (MWs) of the 22 LuCCRs (29.92 kDa to 64.82 kDa), while their predicted isoelectric points (pI) (except for LuCCR3 and LuCCR12) were below 7, indicating they are acidic proteins. Subcellular localization predictions revealed that most LuCCRs were located within chloroplasts, followed by cytoplasmic locations.

Of the 22 *LuCCRs*, 20 were distributed across 9 chromosomes (Fig. 1). Chromosome 7 harbored the most *LuCCR* genes (5), followed by chromosome 1 (4) and chromosome 12 (3). The remaining chromosomes each contained 1–2 *LuCCR* genes. However, *LuCCR21/22* were located on unassembled chromosomal scaffolds, preventing their precise chromosomal localization.

### Sequence homology and phylogenetic analyses of LuCCRs

Homology analysis of LuCCR proteins, conducted using blastp, revealed homologies between LuCCRs 1–22 and functional CCRs of other plants ranging from 35 to 84% (Supplementary Table 2). Among them, LuCCR7/13/15/20 exhibited the highest homologies to known functional CCRs (56-84%). To further study the sequences of LuCCRs, multiple sequence analysis of CCR sequences of *A. thaliana*, *P. tomentosa*, *S. bicolor* and *L. leucocephala* alongside LuCCRs was conducted using DNAMAN software. Sequence alignment results showed that all predicted LuCCRs contained the characteristic primary formations of CCRs, including the representative NAD(P)-binding (NAD(P)-B) Rossmann fold and the conserved Ser-Tyr-Lys (SYK) catalytic triad (Fig. 2) [21, 38]. Moreover, both LuCCRs and CCRs in

**Table 1** Basic information and subcellular localization of *LuCCRs* gene

| Gene name | Gene ID | Length(aa) | MV (kDa) | pI | Aliphatic index | subcellular localization |
|---|---|---|---|---|---|---|
| *LuCCR1* | L.us.o.m.scaffold6.568 | 321 | 35.70 | 5.73 | 88.32 | Cytoplasmic |
| *LuCCR2* | L.us.o.m.scaffold287.5 | 341 | 37.52 | 5.84 | 84.90 | Cytoplasmic |
| *LuCCR3* | L.us.o.m.scaffold73.166 | 513 | 56.10 | 7.85 | 82.03 | Chloroplast |
| *LuCCR4* | L.us.o.m.scaffold73.165 | 275 | 29.92 | 6.75 | 93.96 | Chloroplast |
| *LuCCR5* | L.us.o.m.scaffold22.313 | 335 | 37.37 | 6.3 | 86.09 | Chloroplast |
| *LuCCR6* | L.us.o.m.scaffold96.220 | 332 | 36.23 | 5.26 | 89.31 | Chloroplast |
| *LuCCR7* | L.us.o.m.scaffold2.334 | 342 | 38.13 | 6.36 | 91.70 | Chloroplast |
| *LuCCR8* | L.us.o.m.scaffold251.35 | 324 | 35.95 | 6.02 | 90.80 | Cytoplasmic |
| *LuCCR9* | L.us.o.m.scaffold251.37 | 593 | 64.82 | 5.38 | 96.00 | Nuclear |
| *LuCCR10* | L.us.o.m.scaffold256.56 | 314 | 34.25 | 5.37 | 96.53 | Extracellular |
| *LuCCR11* | L.us.o.m.scaffold100.124 | 320 | 34.71 | 6.18 | 100.81 | Chloroplast |
| *LuCCR12* | L.us.o.m.scaffold23.319 | 330 | 36.26 | 8.07 | 95.42 | Cytoplasmic |
| *LuCCR13* | L.us.o.m.scaffold65.106 | 436 | 47.66 | 6.20 | 90.55 | Chloroplast |
| *LuCCR14* | L.us.o.m.scaffold65.259 | 325 | 35.85 | 6.13 | 93.26 | Cytoplasmic |
| *LuCCR15* | L.us.o.m.scaffold95.70 | 295 | 32.77 | 6.21 | 92.44 | Chloroplast |
| *LuCCR16* | L.us.o.m.scaffold96.89 | 323 | 35.69 | 5.88 | 94.77 | Extracellular |
| *LuCCR17* | L.us.o.m.scaffold139.19 | 332 | 36.29 | 5.57 | 89.01 | Chloroplast |
| *LuCCR18* | L.us.o.m.scaffold3.479 | 325 | 35.24 | 6.61 | 91.17 | Chloroplast |
| *LuCCR19* | L.us.o.m.scaffold71.59 | 287 | 31.96 | 5.59 | 93.69 | Chloroplast |
| *LuCCR20* | L.us.o.m.scaffold63.31 | 344 | 37.70 | 5.82 | 84.16 | Cytoplasmic |
| *LuCCR21* | L.us.o.m.scaffold251.85 | 324 | 35.71 | 5.49 | 88.43 | Cytoplasmic |
| *LuCCR22* | L.us.o.m.scaffold251.87 | 324 | 35.86 | 6.20 | 88.40 | Cytoplasmic |

Length (aa) represents the number of amino acids in the protein encoded by the LuCCRs. MW represents the molecular weight of the LuCCRs protein. pI represents the isoelectric point of the LuCCRs protein. The aliphatic index refers to the abundance and relative content of nonpolar amino acids (such as alanine, valine, isoleucine, and leucine) in proteins

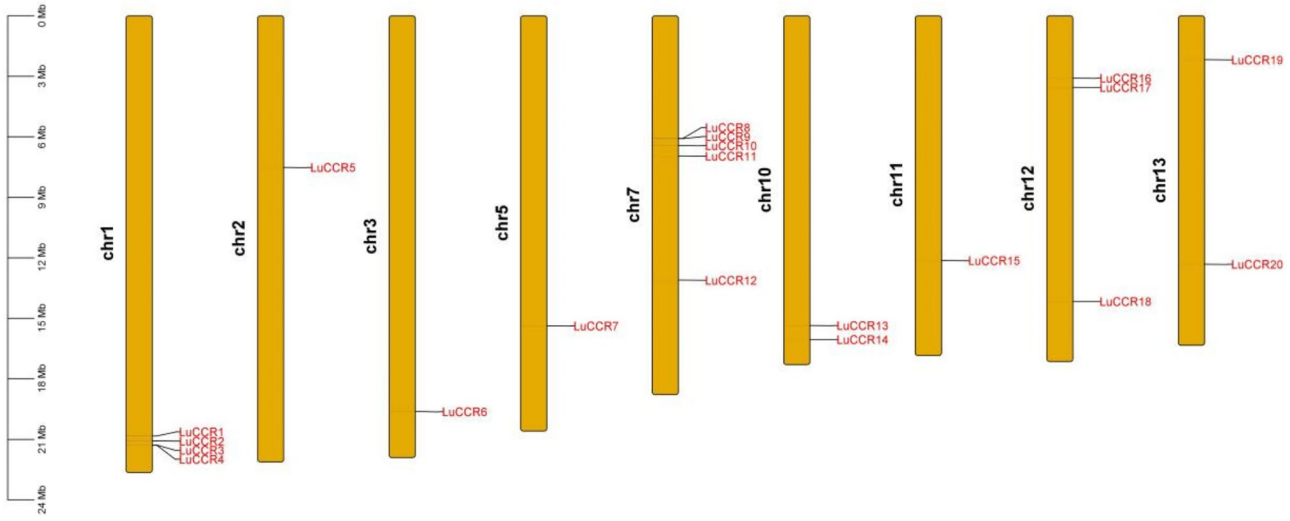


**Fig. 1** Chromosomal location of *CCR* gene family in *Linum usitatissimum*. A chromosome distribution map was drawn based on the physical location of the *LuCCRs* gene on the chromosome. Each vertical bar represents a chromosome. The chromosome number is shown on the left side of each chromosome.The black line on the chromosome indicates the physical location of the *LuCCR* gene

other plant species contained conserved NAD(P)-B and substrate catalysis motifs (Fig. 2), including the CMs G(X)2G(X)2 A/G and D(X)2D, which are involved in NAD(P)-B and adenine-binding pocket stability [21, 37].

Interestingly, the NADP specificity motif R(X)5 K, which is crucial for identifying CCRs from other SDRs depended on NAD(H) [21], was present in all LuCCRs except LuCCR6/16/17/19, while the R(X)6 K motif was present in most LuCCRs. Notably, the possible importanter for CCR activity, CCR signature motif (NWYCYGK), was found in all LuCCRs in the form Y-X-X-X-K except for LuCCR7/13/15/20, which contained the complete NWYCYGK motif.

Analysis of NJ phylogenetic trees of LuCCRs and other plant CCRs revealed their phylogenetic relationships, showing that CCRs could be grouped as two clades: the CCR-like clade (background green) and CCR bona fide clade (CCRBFC, background yellow) (Fig. 3). The CCRBFC could be further divided as two subgroups, a monocot clade and a dicot clade. LuCCR7/13/15/20 clustered with functional dicotyledonous CCRs, such as CCRs of *A. thaliana* and *P. tomentosa* associated with lignin biosynthesis (LB). The CCR-like clade was separated into three subgroups (Group a, Group b and Group c). Group a contained 3 LuCCRs (LuCCR6/16/17), 2 AtCCRs and 2 PtoCCRs, while Group c contained 3 AtCCRs (and no LuCCRs) and Group b contained the remaining LuCCRs.

### Gene structure and CM analysis of *LuCCRs*

Structures at gene level of *LuCCRs* were elucidated through the approach shown in Fig. 4. Based on the count of exons, the 22 *LuCCR* genes were categorized into four groups, with similar structures generally observed within the same group. For example, all members of the second group, comprised of *LuCCR7/13/15/20*, contained five exons. In contrast, genes in the third group contained six exons, while those in the first group featured 2–3 exons and those in the fourth group contained 8–10 exons, highlighting the structural diversity across the four groups.

The MEME online tool was employed to analyze LuCCR protein structures, unveiling 10 cm present across the 22 LuCCRs (Fig. 5). Most of these proteins contained motifs 1–9, while the CCR signature motif was present in all 22 LuCCRs. Motif 2, the NAD(P)-binding motif G(X)2G(X)2 A/G, was identified in all LuCCRs except LuCCR12, while Motif 10 was exclusive to LuCCR7/13/15/16/20.

### CISAE analysis in promoters of *LuCCRs*

To investigate the function and regulatory patterns of the *LuCCR* genes, we predicted cis-acting elements (CISAEs) within a 2000-bp region upstream of the initiation codon of each flax *CCR* gene (Fig. 6A). Except for *LuCCR1*, the remaining 21 *CCR* genes possessed CISAEs ranging from 7 to 30 in number, categorized into four types, including stress-responsive, light-responsive, hormone-responsive and other related elements (Fig. 6B).

*LuCCR* promoters were found to be rich in hormone response elements, such as the abscisic acid (ABA) response element (ABRE) and the methyl jasmonate (MeJA) response element (CGTCA-motif, TGACG-motif). Stress response elements ARE and LTR, which respond to anaerobic induction and low-temperature stress, respectively, were also identified. Additionally, a large number of widely distributed light-responsive elements were found, including ACE, G-box, Sp1 and

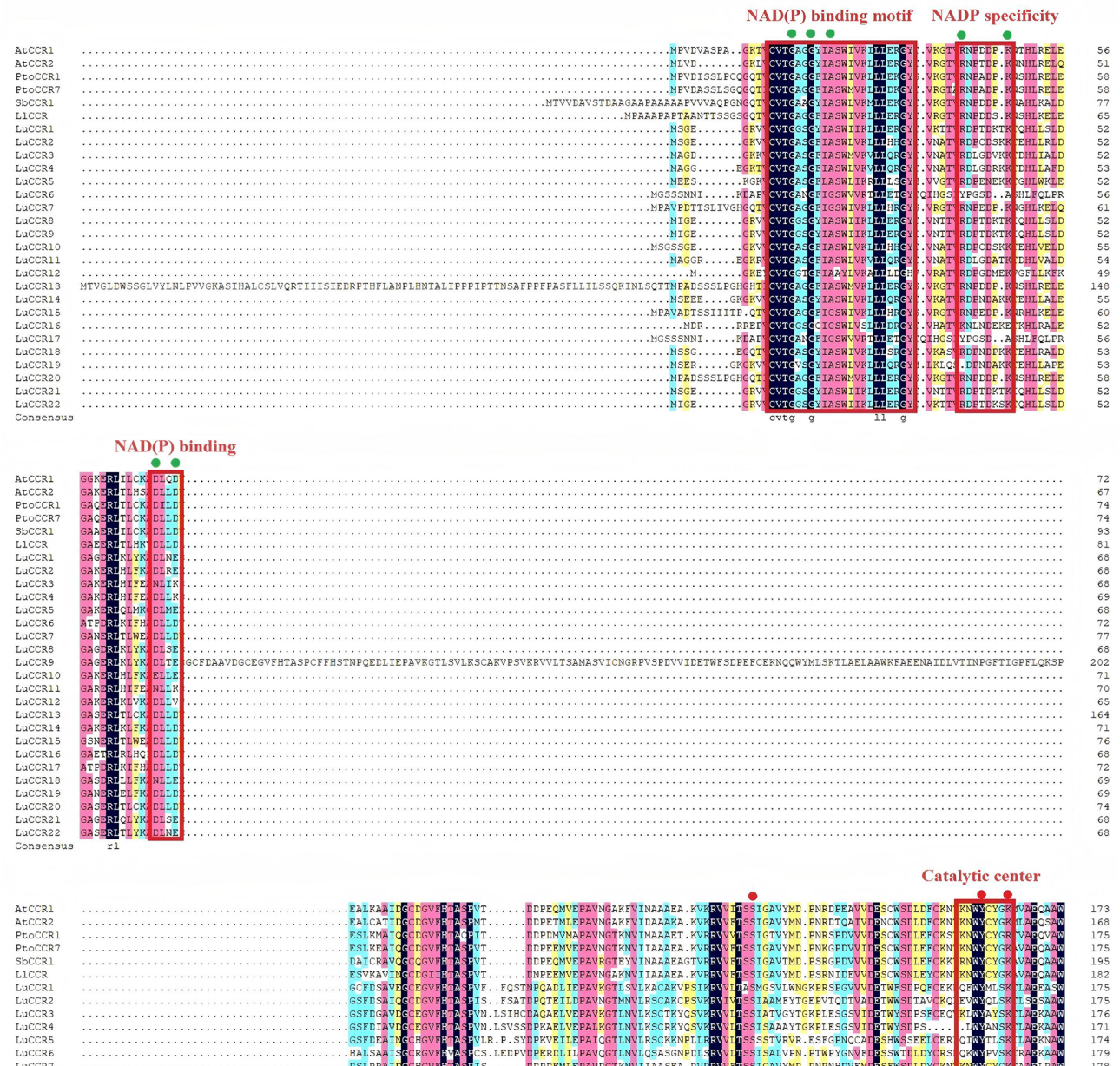


**Fig. 2** MSA of LuCCRs and other plant CCRs. Details for AtCCR1, AtCCR2, PtoCCR1, PtoCCR7, SbCCR1, and LlCCR are listed in Supplementary Table 3. The NAD(P)-B motif, NAD(P) specificity motif, and the catalytic signature motif of CCRs are marked with red boxes. The green dots indicate G(X)2G(X)2 A/G, R(X)5 K and D(X)2D motifs, while the red dot indicates the catalytic triad SYK

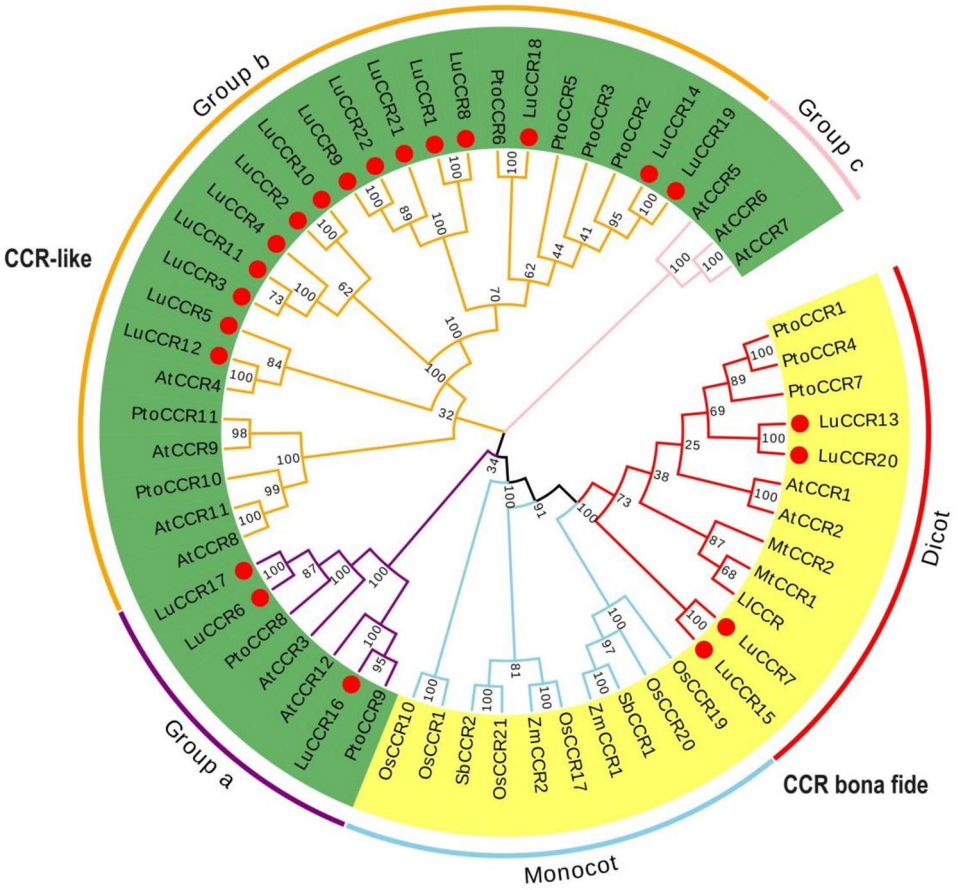


**Fig. 3** Phylogenetic trees of flax CCRs and other plant CCRs. The yellow background indicates the CCR bona fide clade and the green background indicates the CCR-like clade. Lines of different colors represent the different subgroups: red, Dicot; blue, Monocot; purple, Group a; orange, Group b; pink, Group c. The red dots represent LuCCRs. Sequences used to present the phylogenetic tree are in Supplementary Table 4

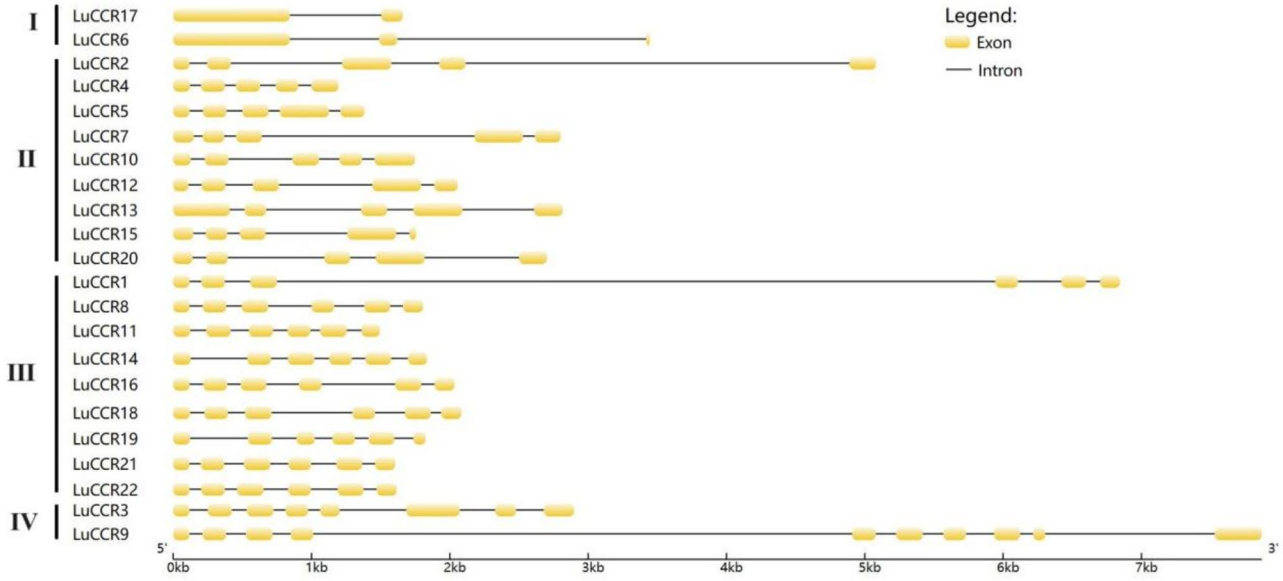


**Fig. 4** .Gene structure of *LuCCRs*. The yellow box shows exons and the black line shows introns

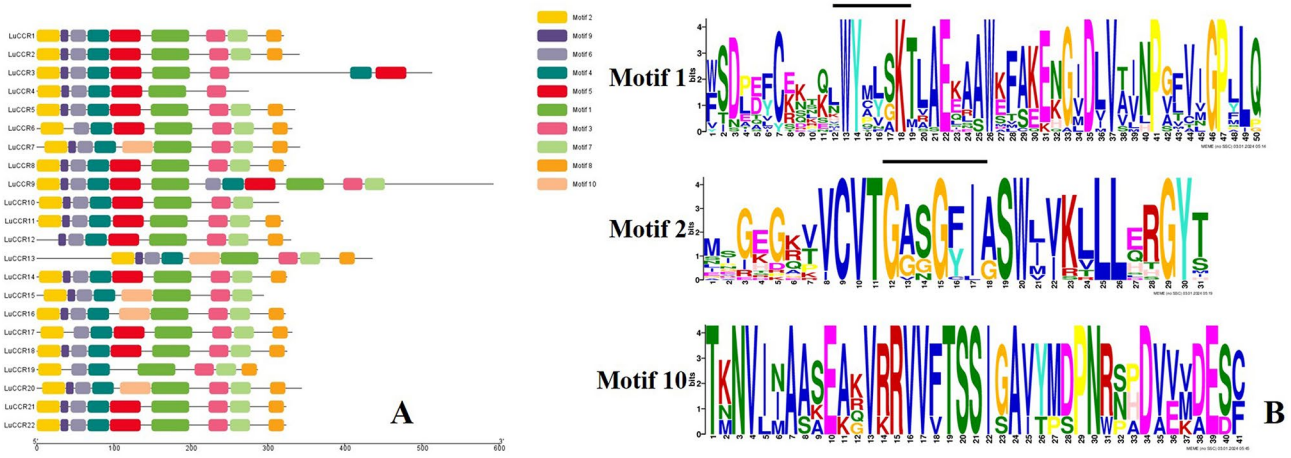


**Fig. 5** Conserved motifs of LuCCR proteins. **A**: Motif composition of LuCCR proteins. Different colored boxes indicate different motifs. **B**: Sequence logos for the three key conserved motifs in the LuCCR protein. CCR signature motif WYCYGK and NAD(P) binding motif G(X)2G(X)2 A/G are marked by solid bars

GT1-motif elements, with the G-box element appearing most frequently, found in 16 promoters.

In addition to these elements, some promoters contained MYB binding sites, which have been implicated in drought and light responses. These data suggest potential roles of *LuCCR* genes in growth, developmental and stress responses in flax.

#### Collinearity analysis of *LuCCR* gene family members

Gene family expansion typically arises from gene duplication issues. To investigate the amplification mechanism of the *LuCCR* gene family, gene duplication events in *L. usitatissimum* were analyzed using MCScanx. Ultimately, a total of 9 segmental duplicated gene pairs were identified across 7 chromosomes of the flax genome (Fig. 7A): *LuCCR1-LuCCR13*, *LuCCR1-LuCCR8*, *LuCCR1-LuCCR20*, *LuCCR2-LuCCR20*, *LuCCR6-LuCCR17*, *LuCCR7-LuCCR15*, *LuCCR8-LuCCR13*, *LuCCR11-LuCCR19 and LuCCR14-LuCCR19*. These findings underscore the significant role of segmental duplication in the expansion of the *LuCCR* gene family.

To delve deeper into the evolutionary correlations of *LuCCR* gene family members, we conducted collinearity analysis on the *CCR* genes of *L. usitatissimum* and two representative species, *A. thaliana* and *O. sativa* (Fig. 7B). Seven pairs of colinear genes were isolated between *L. usitatissimum* and *A. thaliana*, while only one colinear gene pair was found between *L. usitatissimum* and *O. sativa*. These results suggest a closer evolutionary relationship between flax and dicotyledonous plants than with monocotyledonous plants.

#### *LuCCR* genes expression pattern analysis

We examined the expression patterns of *LuCCR* genes across various tissues and developmental stages of flax using RNA-seq transcriptome data (Fig. 8, Supplementary Table 5). The results revealed that nearly half of the *LuCCR* genes, including *LuCCR3/4/5/12/19*, exhibited loexpression levels or no expressed at all in different tissues across different developmental stages (Fig. 8). In contrast, several *LuCCRs (LuCCR9/10/13/14/18/20/22)* showed high expression levels in various tissues during different developmental stages.

Notably, *LuCCR9* and *LuCCR10* were expressed in leaves, stems and roots, with highest expression levels observed in leaves (Fig. 8A). The expression patterns of *LuCCR13/14/18/20* were similar across roots, stems and leaves. However, *LuCCR13/20* exhibited significantly higher expression levels in lignifying organs (such as roots and stems) compared to *LuCCR14/18* (Fig. 8A).

The expression patterns of *LuCCR13/20* remained consistent across different developmental stages and across different parts of stems, indicating robust transcript accumulation. The expression levels of *LuCCR13/20* increased as development progressed, peaking during the fast-growing stage and gradually decreasing thereafter (Fig. 8C). *LuCCR13/20* exhibited high expression in mature stems (S10-S20), while expression in young stems (S1-S3) was low (Fig. 8B). Although *LuCCR13/20* expression was not specific to xylem, these genes were predominantly expressed in lignin-forming tissues, such as stems, suggesting they play crucial roles in lignin synthesis.

#### *LuCCR* genes expression patterns under hormone and abiotic stresses

This study further analyzed the response of the *LuCCR* genes to different hormones and stressors based on transcriptome data (Fig. 9, Supplementary Table 6). The Protein levels of *LuCCR2/6/8/9/10/13/16/17/20/21* were upregulated after treatment with exogenous Gibberellin 3 ($GA_3$). Notably, the promoters of a subset of these genes, *LuCCR6/9/10/13/17/20*, contained GA response

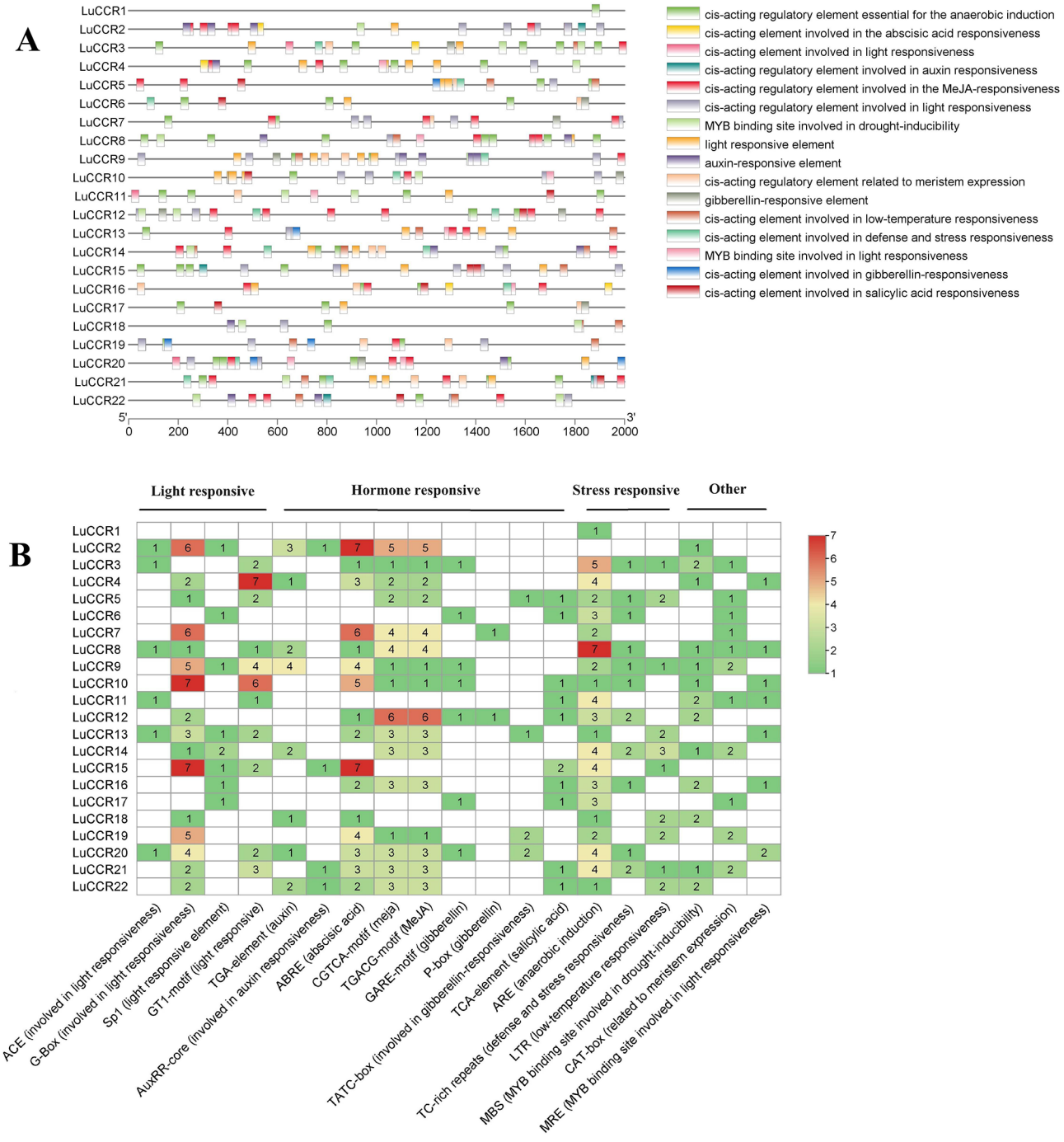


**Fig. 6** Analysis of cis-acting elements of the *LuCCRs* promoter. **A**: Location of different cis-acting elements in the *LuCCRs* promoter. Different color blocks represent different cis-acting elements. **B**: The number of different cis-acting elements in each *LuCCRs* promoter

elements (Fig. 6B), suggesting their involvement in the GA signaling pathway. Following auxin treatment, the expression levels of 12 of 15 *LuCCRs* were upregulated, of which the promoters of *LuCCR2/9/14/18/20/22* harbored auxin response elements (Figs. 6B and 9).

Compared with the control group, upregulated expression of *LuCCR2/10/11/17/21* was observed after NaCl treatment, with *LuCCR2/10/17* showing expression increases of 119%, 97% and 112%, respectively. Similarly, upregulated expression of *LuCCR2/10/11/17/21* was observed after NaOH treatment, while following drought treatment, expression levels of *LuCCR2/5/10/15/17/18* were up-regulated by 39-362%. These results collectively suggest that *LuCCR2/5/10/18* might play pivotal roles in plant abiotic stress tolerance.

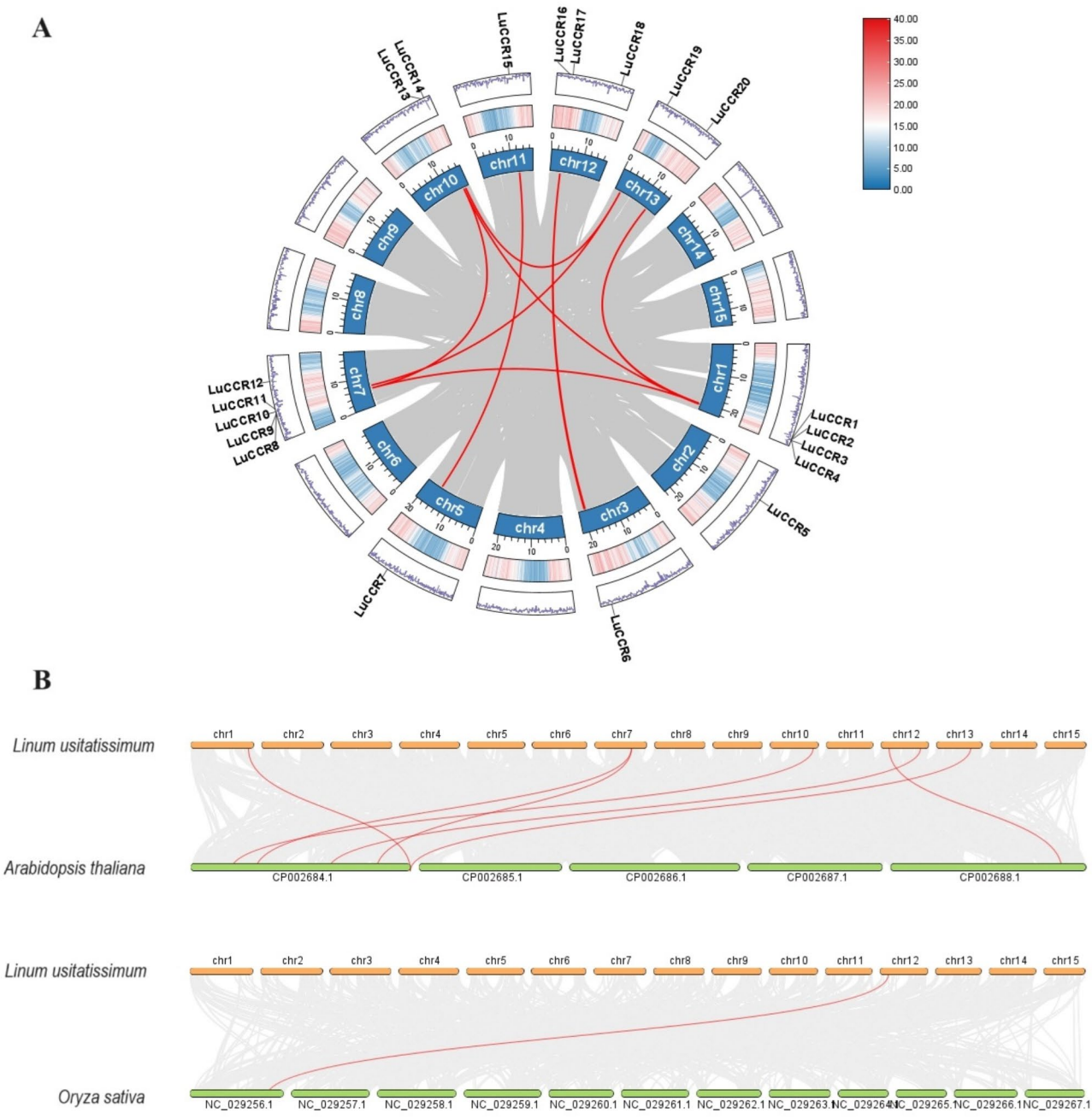


**Fig. 7** Collinearity analysis of *LuCCR* genes. **A**: Syntenic analysis of *CCR* genes in *L. usitatissimum*. **B**: Collinearity of *LuCCR* genes with *CCR* genes in *A. thaliana* and *O. sativa*. The gray lines represent all collinear *CCR* gene pairs, while red lines represent collinear *LuCCR* gene pairs

### qRT-PCR (Quantitative RT-PCR) analysis of *LuCCR* genes expression levels

We conducted qRT-PCR to determine expression levels of *LuCCR14/18/20* in various parts of flax stems. The data presented that these three genes were all expressed in the whole tested tissues, with *LuCCR14/18* exhibiting high-level expression in young stems (S1) followed by slightly lower but stable expression thereafter, as found in mature stems. *LuCCR20* exhibited high-level expression along the stem that decreased slightly as the stem matured. In addition to these three *CCR* genes, three additional genes were randomly selected and the findings demonstrated that expression trends of all six genes were generally consistent with the RNA-seq analysis results, affirming the reliability of the transcriptome results (Fig. 10).

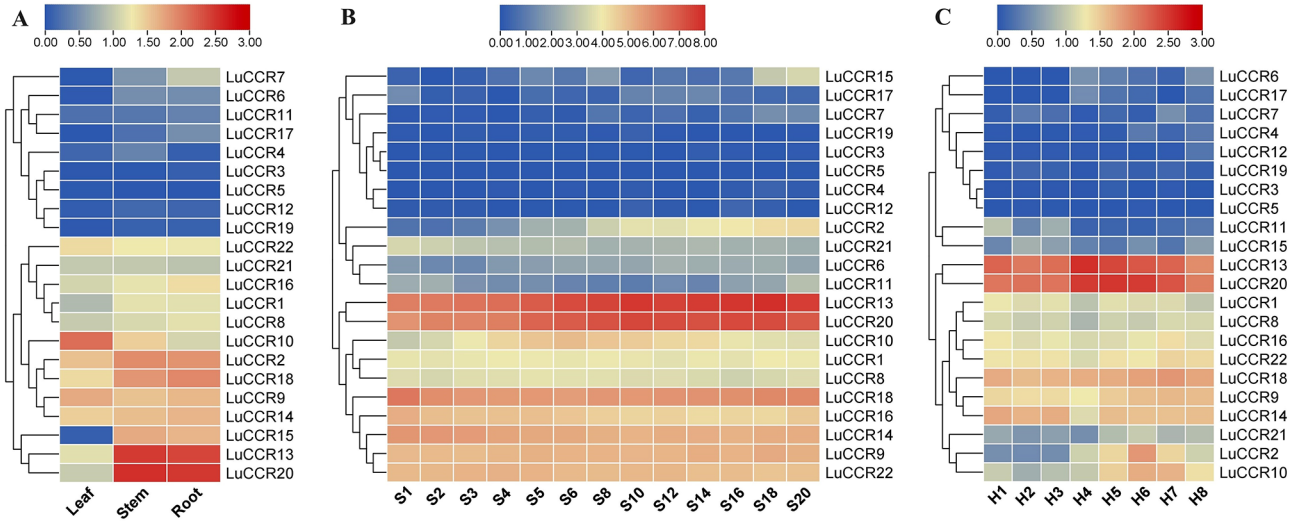


**Fig. 8** Expression pattern of *LuCCRs* gene in *Linum usitatissimum*. **A**: Root, stem and leaf in the fast-growing stage; **B**: different parts of the stem: flax stems of fast-growing stage were divided into 20 equal parts that were named S1-S20. S1 is closest to the shoot apex, and S20 is closest to the root. **C**: Different developmental stages: H1 seedling stage, H2 fir-like stage, H3 early fast-growing stage, H4 fast-growing stage, H5 bud stage, H6 flowering stage, H7 green stage, and H8 maturity stage

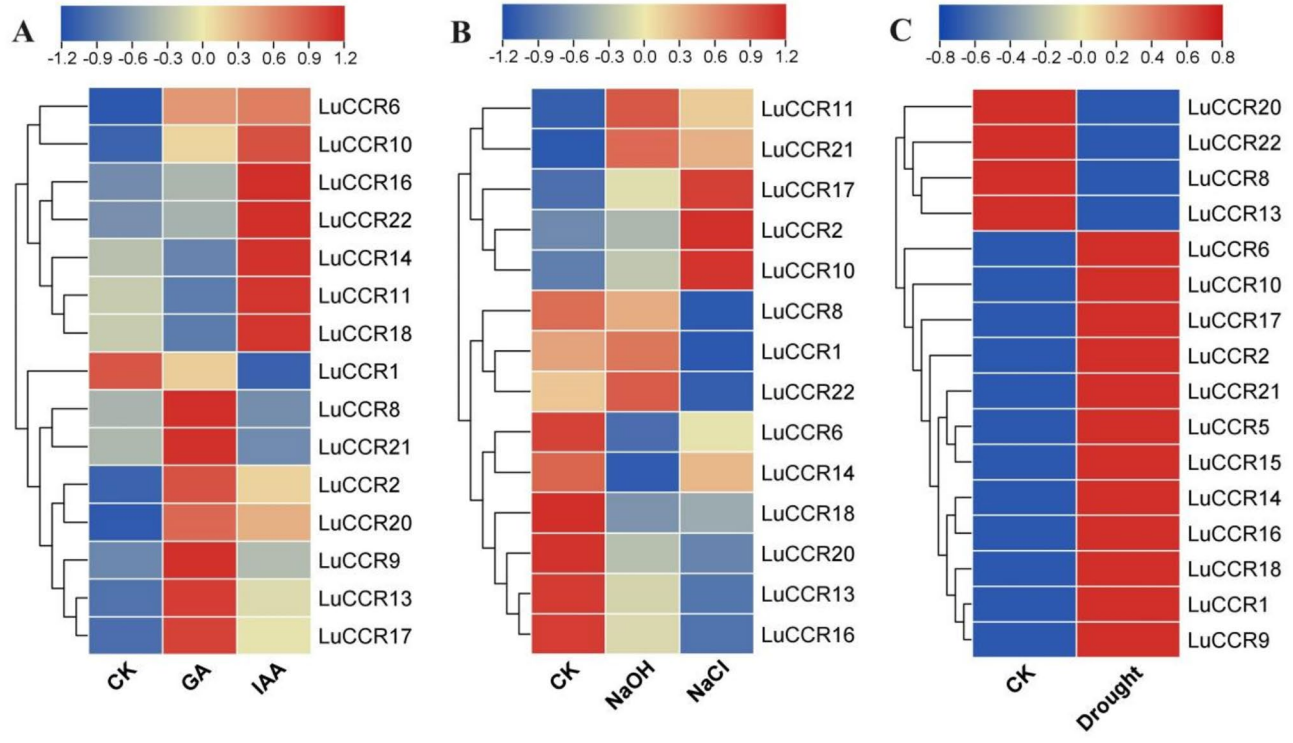


**Fig. 9** Expression patterns of *LuCCRs* in response to various abiotic stresses. **A**: hormone treatment; **B**: NaOH and NaCl treatment; **C**: drought treatment. The heatmap was drawn with TBtools based on transcriptome data, and $\log_{10}$ fold change and row normalization were performed

## Discussion

With the expanding availability of plant genome resources, genome-wide identification has become crucial for elucidating the biological functions of key enzymes and their family members. LB, initiated with the phenylpropanoid pathway, relies on activities of a series of enzymes, with CCRs acting as the primary committed enzymes in the monolignol pathway branch of the LB pathway. First identified in *Eucalyptus gunnii*, *CCR* genes have garnered increasing attention as potential targets of interventions aimed at reducing lignin content in plants [39]. Given the significant impact of lignin content

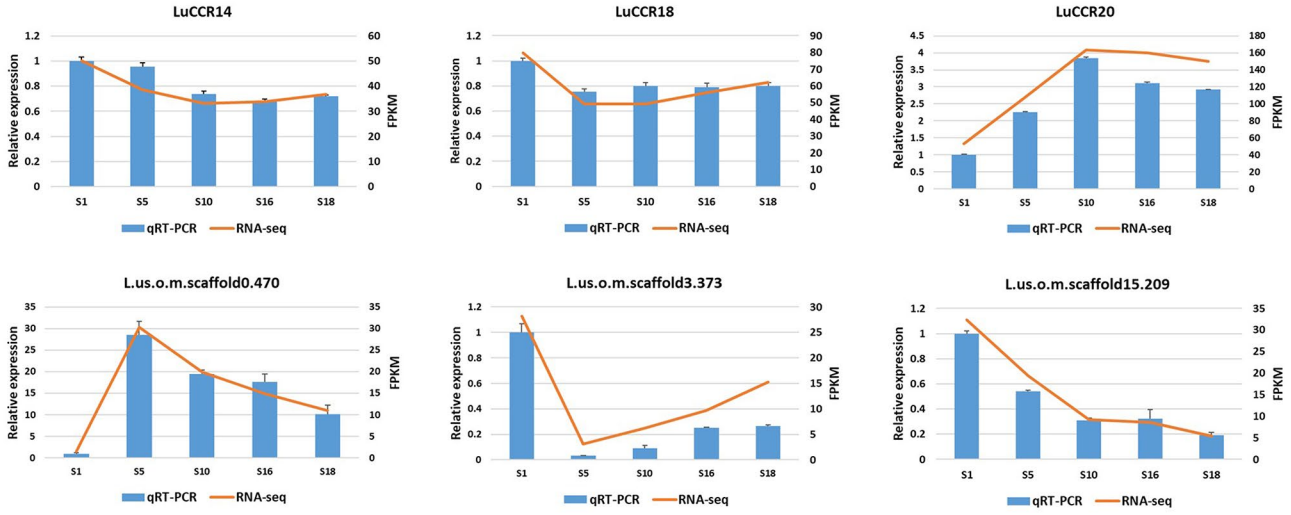


**Fig. 10** Validation of RNA-seq data by qRT-PCR. Flax stems of fast-growing stage were divided into 20 equal parts that were named S1-S20. S1 is closest to the shoot apex, and S20 is closest to the root. Five parts were selected for the qRT-PCR verification. Each gene was normalized with S1 as the control

on flax quality and degumming process, flax breeding to reduce lignin content remains a crucial research priority.

Plant *CCR* genes, often found in gene families, exhibit quantitative diversity across plant species, such as in *A. thaliana* [20], *P. tomentosa* [21], *E. grandis* [24], *Dalbergia odorifera* [37], *M. sativa* [23] and *O. sativa* [22]. This research selected 22 *CCR* genes, a number similar to that identified in *D. odorifera*. The proteins encoded by these *LuCCR* genes exhibited physicochemical properties akin to known functional CCRs [19, 22, 39, 40]. However, exceptions were observed with LuCCR3 and LuCCR9, which displayed unusually long peptide lengths, each containing two domains, unlike previously characterized CCRs in other plants that typically feature a single domain [26, 40, 41]. Furthermore, *LuCCR* distribution was uneven across the central chromosome regions, clustering predominantly at chromosome ends, mirroring observations in *D. odorifera* [37].

All 22 LuCCRs exhibited high homology with the (NAD(P)-B) domain of functional CCRs (Fig. 2), a finding consistent with characteristics shared by members of the SDR family depended on NAD(P)H [21]. Notably, the signature CCR motif NWYCYGK, representing the CCR catalytic active site [21, 39], was entirely conserved in LuCCR7/13/15/20. Additionally, previous studies have shown that the second and third amino acids within this motif, W and Y, respectively, are crucial for enzyme-substrate binding [42], consistent with the extremely high conservation of these residues in all 22 LuCCRs.

The NADP specificity motif R(X)5 K, a pivotal characteristic distinguishing CCR from SDRs depended on NAD(P)H, is highly conserved in active CCRs, such as OsCCR19/20 and PtoCCR1/7 [14, 21, 22]. However, LuCCR6/16/17/19 lacked this motif, while the remaining LuCCRs contained R(X)6 K instead of R(X)5 K, potentially influencing NADPH utilization.

*CCR* and *CCR-like* genes in plant exhibit variable numbers of introns and exons. The *LuCCRs* identified in this study displayed six exon-intron patterns categorized into four classes. Of note, most functional *CCRs* involved in lignification, such as *EuCCR* [39], *AtCCR1* [40], *LlCCR* [28] and *ZmCCR1* [43], harbor 5 exons and 4 introns, the pattern found in *LuCCR7/13/15/20*. However, unlike the *CCR* genes involved in developmental lignification, stress-related *AtCCR2*, *ZmCCR2*, and *SbCCR2-2* exhibit different exon-intron patterns. *AtCCR2* and *ZmCCR2* each consist of four exons, whereas *SbCCR2-2* is composed of six exons [40, 44, 45]. All of the *LuCCR2*, *LuCCR5*, and *LuCCR10* in this study consist of five exons, which differs from previous studies and is largely related to the differences in species.

Genomes of the majority morden plants in land, including the whole vascular plants, are discovered to harbor at least one functional CCR, a prerequisite for tissue lignification [42]. The phylogenetic analysis of this study showed that CCRs involved in developmental lignification were grouped separately from those involved in defense-related processes (Fig. 3). LuCCR7/13/15/20 displayed close evolutionary relationships with PtoCCRs, AtCCRs, MtCCRs and LlCCRs involved in lignification occurring during dicotyledonous plant development. The study found that during development, this group's CCRs display high-level expression, particularly in nascent xylem tissues within stems and roots. For example, in *A. thaliana*, *AtCCR1* was preferentially expressed in stem tissues undergoing lignification [40], which aligns with findings in *L. leucocephala* showing high-level *LlCCR* expression in lignified roots and stems, but not in leaves [46]. In this present study, we discovered the

highest expression levels of *LuCCR13/20* in stems followed by roots. Moreover, the functional *CCR OsCCR20* in rice, which was highly expressed across all developmental stages [22], resembled trends observed herein for *LuCCR13/20* showing high-level expression throughout flax development. Notably, *LuCCR13/20* expression levels gradually increased during stem maturation, aligning with previously reported findings in corn showing high-level *ZmCCR1* expression in stems [44]. These findings collectively suggest that *LuCCR13/20* likely serve as functional *CCRs* that actively participate in flax developmental lignification processes.

Lignification functions as a pivotal defense mechanism against environmental stress, as shown in prior investigations underscoring the roles of CCRs in stress response pathways, including a study demonstrating increased *AtCCR2* mRNA levels following inoculation of *A. thaliana* plants with pathogenic bacteria [40]. Similarly, *HcCCR2* expression in kenaf (*Hibiscus cannabinus*) surged following drought and NaCl treatments [47], while *SbCCR2-1* exhibited elevated expression levels following drought exposure or sorghum aphid infestation [45]. Furthermore, rice *OsCCR10* transcript levels increased after plants were exposed to the hormone ABA or abiotic stressors, such as drought and high salinity [26]. Moreover, our transcriptomic analysis findings revealed upregulated expression of *LuCCR2/10* following both NaOH and NaCl stress treatments, while *LuCCR5/18* expression levels were up-regulated 361% and 72%, respectively, under drought conditions. *LuCCR5* displaying negligible expression in ormally growing tissues and is only induced by drought. These findings collectively suggest potential roles for *LuCCR2/5/10/18* in stress-induced lignification. Unlike previous studies, the LuCCR2/5/10/18, involved in stress response in this study, did not cluster with AtCCR2, SbCCR2, or OsCCR10. Instead, they clustered separately within the CCR-like clade, which may be related to gene duplication during the evolutionary process.

Transgenic technology has been widely applied to control the lignin content and composition of various plants. Notably, downregulation of *AtCCR1* in *A. thaliana* resulted in decreased lignin content of up to 50% [25], while specific reintroduction of *CCR1* in *AtCCR1* mutants effectively mitigated vascular collapse and led to a 59% increase in total stem biomass production compared to WT plants [31]. Similarly, the introduction of *LlCCR* antisense constructs into the AS17 *Nicotiana tabacum* (tobacco) line led to downregulated *CCR* expression resulting in a 24.7% reduction in lignin content, accompanied by a 15% increase in cellulose content. Conversely, lines with upregulated *CCR* expression exhibited significantly increased lignin content [28]. Additionally, in transgenic rice group vs. non-transgenic controls, the over-expressing *OsCCR10* exhibited enhanced drought tolerance during vegetative growth stages, whereas *OsCCR10* knock-out mutants mediated by CRISPR/Cas9 displayed decreased root lignin accumulation and substantially decreased drought tolerance compared to WT controls [26]. This study has identified *CCRs* related to development and *CCRs* related to stress by analyzing the gene structure, phylogeny, and expression patterns of the *CCR* genes. Consequently, we can develop new flax varieties with enhanced stress resistance and desirable lignin content through the overexpression or knockout of the corresponding *CCR* genes.

These results emphasize the potential applications of the *CCR* gene in flax genetic engineering. In flax, suppressing the expression of functional *CCR* gene can produce varieties with low lignin content, but the stress tolerance of the plants may decrease. Conversely, the induction of *CCR* gene expression by environmental stress may assist in plant defense, yet it could negatively impact the quality of flax fibers. Therefore, using molecular biological means to reduce lignin content, one should also consider the overall quality, which would be very interesting work.

## Conclusion

This study identified 22 *CCR* genes within the *L. usitatissimum* genome, distributed across 9 chromosomes. Through multiple sequence alignment, phylogenetic analysis, and examination of gene structures and CMs, LuCCR13/20 were found to align closely with functional CCRs involved in LB in dicotyledonous plants. Consequently, they share NADP-specificity, NAD(P)-B, and CCR signature motifs with known functional CCRs. Notably, transcriptomic analysis indicated robust expression of *LuCCR13/20* throughout flax development, particularly in tissues undergoing active lignification, such as roots and stems, with heightened expression observed in mature stems. These results suggest the functional involvement of these genes in flax LB. In future work, we can genetically modify *LuCCR13/20* to optimize the content of flax lignin. Moreover, upregulated expression of *LuCCR2/5/10/18* under abiotic stress conditions indicates pivotal roles of these genes in defense-related lignification processes in flax. This research may provide theoretical basis for further investigation on LB and its regulation in flax, also, providing deep theoretical basis for the genetic mechanisms essential lignin synthesis and stress response pathways in this important crop.

## Methods

### Identification and chromosome localization of flax *CCR* genes

To investigate flax *CCR* genes and CCR proteins, we established a local database by downloading genomic and

protein data sourced from the NCBI database (https://www.ncbi.nlm.nih.gov/datasets/genome/GCA_010665275.2/) and figshare database (https://figshare.com/articles/dataset/Annotation_files_for_Longya-10_genome/13614311/3), respectively. Utilizing experimentally verified CCR sequences as query sequences (Supplementary Table 3), we conducted BLAST searches against the *L. usitatissimum* protein database using the threshold, e-value = 1e-5. Putative *L. usitatissimum* CCR (LuCCR) conserved sequence domains were confirmed by the CDD online tool (http://www.ncbi.nlm.nih.gov/Structure/cdd/). Only sequences containing conserved CCR domains, including the CCR signature motif (KNWYCYGK), were included in subsequent multiple sequence alignment (MSA) analysis. ExPAsy online program (https://web.expasy.org/protparam/) [48] was applied to predict the physicochemical properties of LuCCR proteins. WoLF PSORT (https://www.genscript.com/wolf-psort.html) was used to conduct the subcellular localization predictions of LuCCR proteins. Chromosome distribution maps of *LuCCR* genes were generated using TBtools based on their physical locations within chromosomes [49].

#### MSA and phylogenetic analyses of LuCCRs

DNAMAN software was introduced to analyze the protein sequences of LuCCRs and representative CCRs (Supplementary Table 3). Then, MEGA7 software of the Neighbor-Joining (NJ) method was applied to orgnize a phylogenetic tree, and thereafter it's reliability was evaluated by the Bootstrap analysis with 1000 replicates. The Evolview (https://www.evolgenius.info/evolview/) [50] was introduced to display the phylogenetic tree.

#### *LuCCR* gene structure and conserved motif (CM) analyses of LuCCRs

Information regarding the locations of *LuCCR* exons and introns was obtained from flax genome annotation files. After that, TBtools software [49] was applied to present their gene structures. MEME (http://meme-suite.org/tools/meme) was introduced to analyze LuCCRs's CM, select criteria is a motif width of 6 × 50 and a maximum number of identified motifs set to 10. Predicted motifs were visualized using TBtools [49].

#### Prediction of cis-acting elements of *LuCCR* gene promoters

For each *LuCCR* gene, PlantCARE (http://bioinformatics.psb.ugent.be/webtools/plantcare/html/) [51]was applied to investigate the CISAEs at the 2000-bp sequences upstream of the translation start site. The results of this analysis were visualized using TBtools.

#### *LuCCR* gene family's collinearity analysis

We obtained *A. thaliana's* and *O. sativa's* genomes and gene annotation files from NCBI, and thereafter, we further carried out the collinearity analysis by the one-step MCScanX module of TBtools to detect gene duplication events in genomes of flax and other species using default parameters. TBtools [49] was adopted to present the predicted results.

#### Expression pattern analysis of *LuCCRs*

Expression pattern analysis was conducted using the fiber flax variety "Diana" and "Heiya 30"as research material. Flax seeds were obtained from the Industrial Crops Institute of Heilongjiang Academy of Agricultural Sciences (Harbin, China), which were sown in the experimental field and cultivated following natural conditions. For "Diane", flax root, stem and leaf samples were collected with three biological replicates at the fast-growing stage from the fiber flax variety "Diana". The middle third of the stems from "Diana" was also collected at different developmental stages, details were as below: at seedling stage which is characterized by the 4th pair of true leaves unfolded, at fir-like stage, symbolled as the stem length/final length = 10%, at early fast-growing stage, which is characterized by the stem length/final length = 30%, at fast-growing stage, characterized by the stem length/final length = 50%, at bud stage which is symbolled as the flower buds are visible, at flowering stage, 50% of flowers are open, at green stage and seeds appeared green and undeveloped, and at mature stage, plants were fully developed for harvesting of fiber. For "Heiya 30", the flax stems were divided into 20 equal parts (designated S1-S20). S1 is closest to the shoot apex, and S20 is closest to the root. S1-S6, S8, S10, S12, S14, S16, S18 and S20 were collected for each sampling site with two biological replicates. After sampling, specimens were promptly frozen in liquid nitrogen and stored at -80 ℃ for further experiment.

#### Hormonal and abiotic stress treatments

For hormonal treatments, expression pattern analysis was conducted using the fiber flax variety "Heiya 16". The flax plants in the fast-growing stage were treated with $GA_3$ (concentration of 100 mg/L) and IAA (concentration of 30 mg/L), respectively. Treatments were applied by spraying and wetting all leaves of the plants, with distilled water serving as the control. After a 24-h treatment period, the top 2-cm portions of stalks were collected, followed by the liquid-nitrogen-frozen treatment at -80 °C.

For abiotic stress treatments, expression pattern analysis was conducted using the fiber flax variety "Heiya 19". For salt-stress or alkaline-stress, flax seedlings (3 weeks old) were induced with NaCl (50 mM) and NaOH (6 mM, pH 11.6), respectively, with distilled water serving as the control. After 18-h treatment, samples were taken from the entire plant (10 mixed samples). RPKM (reads per

kilobase of exon model per million mapped reads) simultaneously represents the sequencing depth and gene length for the read counts. For drought stress, watering of flax plants in the fast-growing stage was stopped for 10 days, causing initial wilting of leaves, after which entire plants were sampled. Control plants were grown under normal conditions and watered every two days. All sampled materials were quickly liquid-nitrogen-frozen treated at -80 ℃ for subsequent experiments.

### DGE library Preparation and sequencing

The Plant Total RNA Extraction Kit (TIANGEN, China) was applied to extract the total RNA. RNA integrity was validated utilizing 1% agarose gel electrophoresis. NanoDrop 1000 spectrophotometer (Thermo Scientific, USA) was utilized to evaluate the concentration and purity of isolated RNA. Sequencing data was filtered using SOAPnuke(v1.5.2) and RNA-sequencing (RNA-seq) data were analysed.

### RNA extraction and qRT-PCR validation

PrimeScript™ RT reagent Kit with gDNA Eraser (TaKaRa, China) was applied to produce the cDNA through the reverse template of total RNA (1 μg). Thereafter, the reaction volume of qRT-PCR was below: TB Green Premix Ex Taq II (TaKaRa) (20 μl), with PCR conducted using a melting temperature (Tm) of 58 °C. Thermal cycling was carried out using a LightCycler 480 System, with the *GAPDH* and *EF1A* genes serving as internal reference genes [36]. The $2^{-\Delta\Delta Ct}$ method was applied to data evaluation. Primer 5.0 was introduced to generate all primers (Supplementary Table 7).

#### Abbreviations

| | |
|---|---|
| ABA | Abscisic acid |
| ABRE | Abscisic acid response element |
| CCR | Cinnamoyl-CoA reductase |
| CCRBFC | CCR bona fide clade |
| CCRGF | CCR gene family |
| CISAEs | Cis-acting elements |
| CM | Conserved motif |
| FPKM | Fragments per kilobase of transcript per million mapped reads |
| GA | Gibberellin |
| LB | Lignin biosynthesis |
| MeJA | Methyl jasmonate |
| NJ | Neighbor-Joining |
| qRT-PCR | Quantitative RT-PCR |
| SDR | Short-chain dehydrogenase/reductase |
| MSA | Multiple sequence alignment |
| MW | Molecular weights |
| WT | Wild type |

## Supplementary Information

The online version contains supplementary material available at https://doi.org/10.1186/s12864-025-11481-5.

Supplementary Material 1

Supplementary Material 2

Supplementary Material 3

Supplementary Material 4

Supplementary Material 5

Supplementary Material 6

Supplementary Material 7

#### Acknowledgements

The authors thank Hongmei Yuan and Guangwen Wu for their support in this study, as well as their guidance and suggestions on the writing of this manuscript.

#### Author contributions

GW and HY designed the study. XS, DL and YY carried out the data analyses, and drafted the manuscript. LT, LC, LY, ZJ and HY implemented experimental work. QK, SC, LZ and JR were involved in proofreading the manuscript and revised the manuscript. All authors approved the final manuscript.

#### Funding

This work was supported by the Heilongjiang Provincial Scientific Research Institute Scientific Research Business Expense Project (CZKYF2022-1-B026), the National Natural Science Foundation of China (31701480) and the China Agriculture Research System of MOF and MARA (CARS-16-S3).

#### Data availability

In this study, genomic and protein data for the analysis of the cinnamoyl-CoA reductase gene family are available in the NCBI database (https://www.ncbi.nlm.nih.gov/datasets/genome/GCA_010665275.2/) and the figshare database (https://figshare.com/articles/dataset/Annotation_files_for_Longya-10_genome/13614311/3), respectively.

## Declarations

#### Ethics approval and consent to participate

Not applicable.

#### Consent for publication

Not applicable.

#### Competing interests

The authors declare no competing interests.

Received: 5 August 2024 / Accepted: 13 March 2025
Published online: 31 March 2025

#### References

1. Sa R, Yi L, Siqin B, et al. Chromosome-Level genome assembly and annotation of the fiber flax (. Front Genet. 2021;12:735690. https://doi.org/10.3389/fgene.2021.735690.
2. Dmitriev AA, Pushkova EN, Novakovskiy RO, et al. Genome sequencing of fiber flax cultivar Atlant using Oxford nanopore and illumina platforms. Front Genet. 2021;11:590282. https://doi.org/10.3389/fgene.2020.590282.
3. Yuan H, Guo W, Zhao L, et al. Expression characteristics analysis of CesA/Csl genes in flax during the fast growing stage. J Nat Fibers. 2022;19(14):7864–77. https://doi.org/10.1080/15440478.2021.1958418.
4. Povkhova LV, Melnikova NV, Rozhmina TA, et al. Genes associated with the flax plant type (Oil or Fiber) identified based on genome and transcriptome sequencing data. Plants (Basel). 2021;10(12):2616. https://doi.org/10.3390/plants10122616.
5. Liu Q, Luo L, Zheng L, Lignins. Biosynthesis and biological functions in plants. Int J Mol Sci. 2018;19(2):335. https://doi.org/10.3390/ijms19020335.
6. Zhao Q, Lignification. Flexibility, biosynthesis and regulation. Trends Plant Sci. 2016;21(8):713–21. https://doi.org/10.1016/j.tplants.2016.04.006.
7. Duan S, Xu B, Cheng L, et al. Bacterial strain for Bast fiber crops degumming and its bio-degumming technique. Bioprocess Biosyst Eng. 2021;44(12):2503–12. https://doi.org/10.1007/s00449-021-02622-7.

8. Sharma S, Mandhan RP, Sharma J. sp. SPJ: an economic and eco-friendly approach for degumming of flax fibers. World J Microbiol Biotechnol. 2011;27:2697–701. https://doi.org/10.1007/s11274-011-0743-1.
9. Xiang M, Bai Y, Li Y, et al. An eco-friendly degumming process of flax roving without acid pickling and NaClO2-bleaching. Process Biochem. 2020;93:77–84. https://doi.org/10.1016/j.procbio.2020.03.018.
10. Labeeuw L, Martone PT, Boucher Y, et al. Ancient origin of the biosynthesis of lignin precursors. Biol Direct. 2015;10:23. https://doi.org/10.1186/s13062-015-0052-y.
11. Miedes E, Vanholme R, Boerjan W, et al. The role of the secondary cell wall in plant resistance to pathogens. Front Plant Sci. 2014;5:358. https://doi.org/10.3389/fpls.2014.00358.
12. Vanholme R, Demedts B, Morreel K, et al. Lignin biosynthesis and structure. Plant Physiol. 2010;153(3):895–905. https://doi.org/10.1104/pp.110.155119.
13. Goffner D, Campbell MM, Campargue C, et al. Purification and characterization of Cinnamoyl-Coenzyme A:NADP oxidoreductase in. Plant Physiol. 1994;106(2):625–32. https://doi.org/10.1104/pp.106.2.625.
14. Pan H, Zhou R, Louie GV, et al. Structural studies of cinnamoyl-CoA reductase and cinnamyl-alcohol dehydrogenase, key enzymes of monolignol biosynthesis. Plant Cell. 2014;26(9):3709–27. https://doi.org/10.1105/tpc.114.127399.
15. Baltas M, Lapeyre C, Bedos-Belval F, et al. Kinetic and Inhibition studies of cinnamoyl-CoA reductase 1 from. Plant Physiol Biochem. 2005;43(8):746–53. https://doi.org/10.1016/j.plaphy.2005.06.003.
16. Li L, Cheng X, Lu S, et al. Clarification of cinnamoyl co-enzyme A reductase catalysis in monolignol biosynthesis of Aspen. Plant Cell Physiol. 2005;46(7):1073–82. https://doi.org/10.1093/pcp/pci120.
17. Sattler SA, Walker AM, Vermerris W, et al. Structural and biochemical characterization of Cinnamoyl-CoA reductases. Plant Physiol. 2017;173(2):1031–44. https://doi.org/10.1104/pp.16.01671.
18. Sonawane P, Vishwakarma RK, Khan BM. Biochemical characterization of Recombinant cinnamoyl coa reductase 1 (LI-CCRH1) from. Int J Biol Macromol. 2013;58:154–9. https://doi.org/10.1016/j.ijbiomac.2013.03.050.
19. Li W, Hao Z, Yang L, et al. Genome-wide identification and characterization of. Reveals its Potential Role Lignin Biosynth Liriodendron chinense Front Plant Sci. 2023;13:1110639. https://doi.org/10.3389/fpls.2022.1110639.
20. Costa MA, Collins RE, Anterola AM, et al. An in Silico assessment of gene function and organization of the phenylpropanoid pathway metabolic networks in. Limitations Thereof Phytochemistry. 2003;64(6):1097–112. https://doi.org/10.1016/s0031-9422(03)00517-x.
21. Chao N, Li N, Qi Q, et al. Characterization of the cinnamoyl-CoA reductase (CCR) gene family in. Reveals Enzymatic Act Sites Evol CCR Planta. 2017;245(1):61–75. https://doi.org/10.1007/s00425-016-2591-6.
22. Park HL, Bhoo SH, Kwon M, et al. Biochemical and expression analyses of the rice Cinnamoyl-CoA reductase gene family. Front Plant Sci. 2017;8:2099. https://doi.org/10.3389/fpls.2017.02099.
23. Cui W, Zhuang Z, Jiang P, et al. Characterization, expression profiling, and biochemical analyses of the. Gene Family Lignin Synthesis Alfalfa Plants Int J Mol Sci. 2022;23(14):7762. https://doi.org/10.3390/ijms23147762.
24. Carocha V, Soler M, Hefer C, et al. Genome-wide analysis of the lignin toolbox of Eucalyptus grandis. New Phytol. 2015;206(4):1297–313. https://doi.org/10.1111/nph.13313.
25. Goujon T, Ferret V, Mila I, et al. Down-regulation of the. Gene Arabidopsis Thaliana: Eff Phenotype Lignins Cell Wall Degradability Planta. 2003;217(2):218–28. https://doi.org/10.1007/s00425-003-0987-6.
26. Bang SW, Choi S, Jin X, et al. Transcriptional activation of rice. 10 OsNAC5 Contributes Drought Tolerance Modulating Lignin Accumulation Roots Plant Biotechnol J. 2022;20(4):736–47. https://doi.org/10.1111/pbi.13752.
27. Leplé JC, Dauwe R, Morreel K, et al. Downregulation of cinnamoyl-coenzyme A reductase in Poplar: multiple-level phenotyping reveals effects on cell wall polymer metabolism and structure. Plant Cell. 2007;19(11):3669–91. https://doi.org/10.1105/tpc.107.054148.
28. Prashant S, Srilakshmi Sunita M, Pramod S, et al. Down-regulation of. Cinnamoyl CoA Reductase (LICCR) Gene Induces Signif Changes Phenotype Soluble Phenolic Pools Lignin Transgenic Tob Plant Cell Rep. 2011;30(12):2215–31. https://doi.org/10.1007/s00299-011-1127-6.
29. Smith RA, Cass CL, Mazaheri M, et al. Suppression of. Increases Level Monolignol Ferulates Incorporated into Maize Lignins Biotechnol Biofuels. 2017;10:109. https://doi.org/10.1186/s13068-017-0793-1.
30. Zhou R, Jackson L, Shadle G, et al. Distinct cinnamoyl coa reductases involved in parallel routes to lignin in. Proc Natl Acad Sci U S A. 2010;107(41):17803–8. https://doi.org/10.1073/pnas.1012900107.
31. De Meester B, de Vries L, Özparpucu M, et al. Vessel-Specific reintroduction of CINNAMOYL-COA REDUCTASE1 (CCR1) in dwarfed. Mutants Restores Vessel Xylary Fiber Integr Increases Biomass Plant Physiol. 2018;176(1):611–33. https://doi.org/10.1104/pp.17.01462.
32. Yin N, Li B, Liu X, et al. Two types of cinnamoyl-CoA reductase function divergently in accumulation of lignins, flavonoids and glucosinolates and enhance lodging resistance in brassica Napus. Crop J. 2022;10(3):647–60. https://doi.org/10.1016/j.cj.2021.10.002.
33. Wang Z, Hobson N, Galindo L, et al. The genome of flax (. Plant J. 2012;72(3):461–73. https://doi.org/10.1111/j.1365-313X.2012.05093.x.
34. Xie D, Dai Z, Yang Z, et al. Genome-Wide association study identifying candidate genes influencing important agronomic traits of flax (. L) Using SLAF-seq Front Plant Sci. 2018;8:2232. https://doi.org/10.3389/fpls.2017.02232.
35. Guo D, Jiang H, Yan W, et al. Resequencing 200 flax cultivated accessions identifies candidate genes related to seed size and weight and reveals signatures of artificial selection. Front Plant Sci. 2020;10:1682. https://doi.org/10.3389/fpls.2019.01682.
36. Liu D, Yuan H, Yao Y et al. Genome-Wide Identification and Expression Pattern Analysis of the F5H Gene Family in Flax (Linum usitatissimum L.). Agronomy-basel. 2023;13(4):1108. https://doi.org/10.3390/agronomy13041108
37. Wang Y, Xu J, Zhao W, et al. Genome-wide identification, characterization, and genetic diversity of. Gene Family Dalbergia Odorifera Front Plant Sci. 2022;13:1064262. https://doi.org/10.3389/fpls.2022.1064262.
38. Kallberg Y, Oppermann U, Jörnvall H, et al. Short-chain dehydrogenase/reductase (SDR) relationships: a large family with eight clusters common to human, animal, and plant genomes. Protein Sci. 2002;11(3):636–41. https://doi.org/10.1110/ps.26902.
39. Lacombe E, Hawkins S, Van Doorsselaere J, et al. Cinnamoyl coa reductase, the first committed enzyme of the lignin branch biosynthetic pathway: cloning, expression and phylogenetic relationships. Plant J. 1997;11(3):429–41. https://doi.org/10.1046/j.1365-313x.1997.11030429.x.
40. Lauvergeat V, Lacomme C, Lacombe E, et al. Two cinnamoyl-CoA reductase (CCR) genes from. Are Differentially Expressed Dur Dev Response Infect Pathogenic bacteria Phytochemistry. 2001;57(7):1187–95. https://doi.org/10.1016/s0031-9422(01)00053-x.
41. Prasad NK, Vindal V, Kumar V, et al. Structural and Docking studies of. Cinnamoyl CoA Reductase J Mol Model. 2011;17(3):533–41. https://doi.org/10.1007/s00894-010-0744-2.
42. Barakat A, Yassin NB, Park JS, et al. Comparative and phylogenomic analyses of cinnamoyl-CoA reductase and cinnamoyl-CoA-reductase-like gene family in land plants. Plant Sci. 2011;181(3):249–57. https://doi.org/10.1016/j.plantsci.2011.05.012.
43. Tamasloukht B, Wong Quai Lam MS, Martinez Y, et al. Characterization of a cinnamoyl-CoA reductase 1 (CCR1) mutant in maize: effects on lignification, fibre development, and global gene expression. J Exp Bot. 2011;62(11):3837–48. https://doi.org/10.1093/jxb/err077.
44. Pichon M, Courbou I, Beckert M, Boudet AM, Grima-Pettenati J. Cloning and characterization of two maize cDNAs encoding cinnamoyl-CoA reductase (CCR) and differential expression of the corresponding genes. Plant Mol Biol. 1998;38(4):671–6. https://doi.org/10.1023/a:1006060101866.
45. Li J, Fan F, Wang L, et al. Cloning and expression analysis of. (CCR) Genes sorghum PeerJ. 2016;4:e2005. https://doi.org/10.7717/peerj.2005.
46. Srivastava S, Gupta RK, Arha M, et al. Expression analysis of cinnamoyl-CoA reductase (. Pulp Yielding Tree Species Plant Physiol Biochem. 2011;49(2):138–45. https://doi.org/10.1016/j.plaphy.2010.11.001.
47. Ghosh R, Choi B, Cho BK, et al. Characterization of developmental- and stress-mediated expression of cinnamoyl-CoA reductase in Kenaf (. L) ScientificWorldJournal. 2014;2014:601845. https://doi.org/10.1155/2014/601845.
48. Duvaud S, Gabella C, Lisacek F, et al. Expasy, the Swiss bioinformatics resource portal, as designed by its users. Nucleic Acids Res. 2021;49(W1):216–27. https://doi.org/10.1093/nar/gkab225.
49. Chen C, Chen H, Zhang Y, et al. TBtools: an integrative toolkit developed for interactive analyses of big biological data. Mol Plant. 2020;13(8):1194–202. https://doi.org/10.1016/j.molp.2020.06.009.
50. He Z, Zhang H, Gao S, et al. Evolview v2: an online visualization and management tool for customized and annotated phylogenetic trees. Nucleic Acids Res. 2016;44(W1):236–41. https://doi.org/10.1093/nar/gkw370.

51. Lescot M, Déhais P, Thijs G, et al. PlantCARE, a database of plant cis-acting regulatory elements and a portal to tools for in Silico analysis of promoter sequences. Nucleic Acids Res. 2002;30(1):325–7. https://doi.org/10.1093/nar/30.1.325.

## Publisher's note